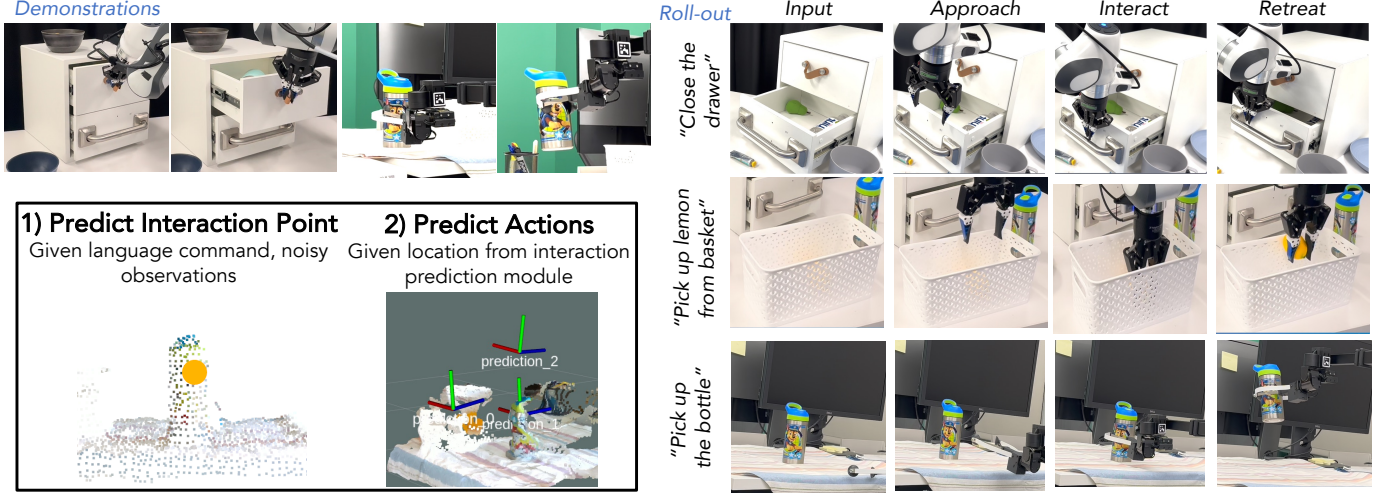


# Spatial-Language Attention Policies for Efficient Robot Learning

Priyam Parashar, Jay Vakil, Sam Powers, and Chris Paxton



**Fig. 1:** We introduce Spatial Language Attention Policies(SLAP), a method for learning from demonstration which works efficiently from very few demonstrations, can handle unstructured 3D scenes, can learn a large number of tasks from a single multi-task policy, and generalizes better to unseen environments and distractors. Our method has two components: an “interaction prediction” module which localizes relevant features in a scene, and an “action prediction” module which uses local context to predict an executable action.

**Abstract**—We investigate how to build and train spatial representations for robot decision making with Transformers. In particular, for robots to operate in a range of environments, we must be able to quickly train or fine-tune robot sensorimotor policies that are robust to clutter, data efficient, and generalize well to different circumstances. As a solution, we propose Spatial Language Attention Policies (SLAP). SLAP uses three-dimensional tokens as the input representation to train a single multi-task, language-conditioned action prediction policy. Our method shows 80% success rate in the real world across eight tasks with a single model, and a 47.5% success rate when unseen clutter and unseen object configurations are introduced, even with only a handful of examples per task. This represents an improvement of 30% over prior work (20% given unseen distractors and configurations). See videos on our website: <https://robotslap.github.io>

## I. INTRODUCTION

Transformers have demonstrated impressive results on natural language processing tasks by being able to contextualize large numbers of tokens over long sequences, and even show substantial promise for robotics in a variety of manipulation tasks [1], [2], [3]. However, when it comes to using transformers for *mobile* robots performing long-horizon tasks, we face the challenge of representing spatial information in a useful way. In other words, we need a fundamental unit of representation - an equivalent of a “word” or “token” - that can handle spatial awareness in a way that is independent of the robot’s exact embodiment. We argue this is essential for enabling robots to perform manipulation tasks in diverse

human environments, where they need to be able to generalize to new positions, handle changes in the visual appearance of objects and be robust to irrelevant clutter. In this work, we propose Spatial-Language Attention Policies (SLAP), that use a point-cloud based tokenization which can scale to a number of viewpoints, and has a number of advantages over prior work.

Our approach, SLAP, tokenizes the world into a varying-length stream of multi-resolution spatial embeddings, which capture a local context based on PointNet++ [4] features. Unlike ViT-style solutions [1], object-centric solutions [5], [3], or 3D features captured on a static grid [2], these PointNet++-based [4] tokens capture free-form relations between observed points in space. This means that we can combine multiple camera views from a moving camera when making decisions and still be able to process arbitrary-lengths of sequences.

Our approach leverages a powerful skill representation we refer to as “attention-driven robot policies” [6], [7], [8], [2], [9] operating on an input-space combining language with spatial information. Unlike other methods that directly predict robot motor controls [10], [1], these techniques predict goal poses in Cartesian space and integrate them with a motion planner [6], [8], [2] or conditional low-level policy [9] to execute goal-driven motion. This approach requires less data, but it still has limitations such as making assumptions about the input scene’s size and camera position and long training times [7], [6], [2]. As in prior work, we aim to use a transformer to make decisions about what actions the robot should take

next [2], using a 3d spatially-organized input space. action representations grounded in scene structure. This approach is a data-efficient way to train generalizable robot behaviors using large-scale transformers. However, these methods fall into a different trap: they make strong assumptions about how big the input scene is [2], where the camera is [7], [6], and generally take a very long time to train [7], [6], meaning they could not be used to quickly teach policies in a new environment.

Specifically, SLAP uses a hybrid policy architecture that incorporates an *interaction prediction* module to determine which parts of the tokenized environment the robot should focus on, and a *relative action* module that predicts parameters of continuous motion with respect to the interaction features in the world. We demonstrate better performance than the current state-of-the-art, PerAct, [2], with 80% success rate on 8 static real-world tasks on held-out scene configurations and a 47.5% success rate tested with out-of-distribution objects. At the same time, we show that SLAP generalizes better to unseen positions and orientations, as well as distractors, while being unrestricted by workspace size, camera placement assumption, using fewer demonstrations and training in roughly a day. We also show SLAP enabling a mobile manipulator, with completely different camera and end-effector configuration from the stationary robot, to execute manipulation trajectories based on a handful of demonstrations.

## II. RELATED WORK

Attention-based policies have been widely studied in prior research and have been found to have superior data efficiency, generalization, and the ability to solve previously unsolvable problems [11], [9], [6], [12], [2], [13]. However, these approaches often rely on strong assumptions about the robot’s workspace, such as modeling the entire workspace as a 2D image [12], [6], [7], [8] or a 3D voxel cube with predetermined scene bounds [2], [9]. This restricts their applicability and may lead to issues related to camera positioning, workspace location, and discretization size. Additionally, these works can be seen, at least partly, as applications of object detection systems like Detic [14] or 3DETR [15], but they lack the manipulation component.

Compared to previous works, some recent studies focus on unstructured point clouds [11], [16]. These approaches demonstrate improved data efficiency and performance compared to traditional behavior cloning. For instance, Where2Act [11] and VAT-Mart [16] predict interaction trajectories, while UMP-Net [17] supports closed-loop 6DoF trajectories. They share a common framework where they have a generalizable methods to predict the interaction location and then predict local motion for the robot.

**Training quickly with attention-based policies.** CLIP-Port [7] and its 3D extension PerAct [2] are attention-based policies that predict attention similar to Transporter Nets [6]. While fitting our definition of attention-based policies, they have limitations as they confine their workspace and treat action prediction as a classification problem in a discrete space. Earlier works, such as SPOT [12], have demonstrated

the usefulness of 2D attention-based policies for fast RL training, including sim-to-real transfer. However, they also have workspace limitations. Nevertheless, Zeng et al. [6] have shown that these policies are valuable for certain real-world tabletop tasks like kitting.

**Language and robotics.** Language is a natural and powerful way to specify goals for multi-task robot systems. Say-Can [10] shows a large-language model that combines sequential low-level skills, many of which are themselves language-conditioned policies. We see our method as a way of quickly creating these low-level skills. RT-1 [1] learns language-conditioned skills, but does not handle clutter or complex scenes. In PaLM-E [3], textual and multi-modal tokens are interleaved as inputs to the Transformer for handling language and multimodal data to generate high-level plans for robotics tasks. Our approach is a spatial extension of this strategy.

**Language for Low-Level Skills.** A number of works have shown how to learn low-level language-conditioned skills, e.g. [7], [2], [1], [18]. Of note is work by Mees et al. [18], which, like our work, predicts 6DoF end effector goal positions end-to-end, and chains them together with large language models. It works by predicting a 2D affordance heatmap and depth from RGB; while we don’t predict depth, we specifically look at robustness and generalization in our work, and theirs is trained from play data in mostly-fixed scenes. Shridhar et al. [2] predict a 3D voxelized grid and show strong real-world performance with relatively few examples, but don’t look at out-of-domain generalization and are limited to a coarse voxelization of the world.

**Vision-Language Navigation.** Similar representations are often used to predict subgoals for exploration in vision-language navigation [19], [20], [8], [21]. HLSM builds a voxel map [19], whereas FiLM builds a 2D representation and learns to predict where to go next [20]. VLMaps proposes an object-centric solution, creating a set of candidate objects to move to [8], while CLIP-Fields learns an implicit representation which can be used to make predictions about point attentions in responds to language queries [21], but does not look at manipulation. Notably, this is a very similar setting to ours, but pretrains a representation on classification and language annotation instead of training on attention and keyframe prediction.

## III. APPROACH

Most robotics manipulation tasks will necessarily involve interacting with the environment [11]. This means that each robot skill will include some interaction point or points. However, in a scene with clutter, it may not be obvious from the scene alone what or where interaction is desired. This means that in realistic settings, it is advantageous to be able to specify a task via natural language.

Combining these assumptions, we imagine a language-conditioned policy  $\pi(x, l)$ , which takes some variable observation  $x$  and a language command  $l$  as inputs and predicts an *interaction point*  $p_I$ , as well as a set of *relative motions*, which

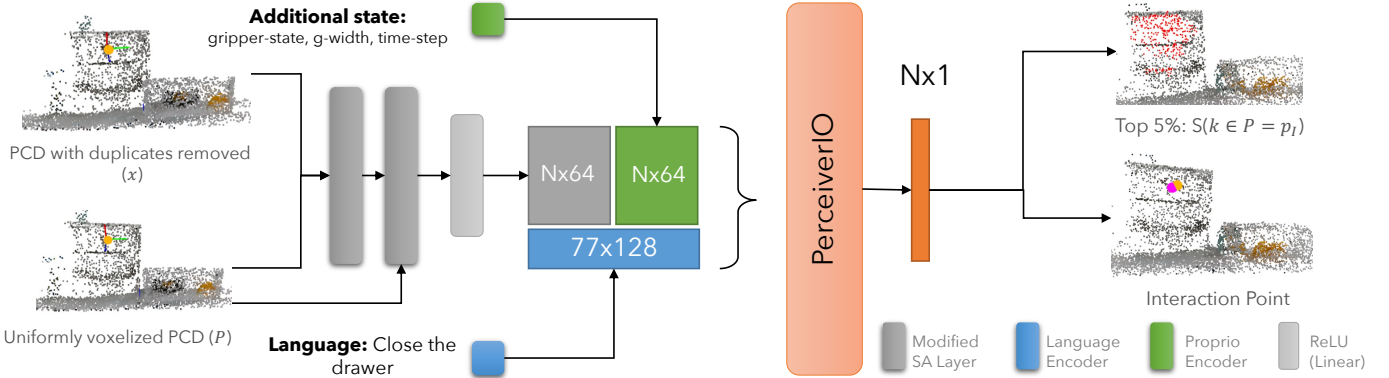


Fig. 2: An overview of the architecture of the interaction prediction module. The point cloud is downsampled to remove duplicates and encoded using two modified set-abstraction layers. The SA layers generate a local spatial embedding which is concatenated with proprioceptive features - in our case, the current gripper state. Both spatial and language features are concatenated and input into a PerceiverIO transformer backbone. We then predict an interaction score per spatial feature and the *argmax* is chosen as the interaction site for command  $l$ .

instead of being in absolute coordinates are offsets from this point.

The interaction point  $p_I$  is predicted by an **Interaction Prediction Module**  $\pi_I$ , and the continuous component of the action by a **Relative Action Module**  $\pi_R$ . The Interaction Prediction Module  $\pi_I$  predicts *where the robot should attend to*; it is a specific location in the world, where the robot will be interacting with the object as a part of its skill. The Relative Action Module  $\pi_R$  predicts a relative action sequence with respect to this contact point in the Cartesian space. These actions are then provided as input to a low-level controller to execute the trajectory. These models are trained using labeled expert demonstrations; a complete process overview is presented in Fig. 3.

#### A. Problem Definition

Given an observation  $x$  of a scene, and a language description  $l$  of an action to execute in this scene, the system outputs a sequence of end-effector actions in Cartesian space and gripper actions:

$$a = (p, q, g)$$

where  $p = (p_x, p_y, p_z)$  is a Cartesian translation relative to the task's predicted interaction point  $p_I$ ,  $q = (q_w, q_x, q_y, q_z)$  is a unit quaternion orientation in the robot's base coordinate frame, and  $g \in \{0, 1\}$  is a gripper action. The scene observation  $x = \{v_0, \dots, v_n\}$  is aggregated from any number of views  $v_i$ , meaning that the actual dimensionality of  $x$  can vary between executions. We train  $\pi_I$  and  $\pi_R$  as multi-task models to predict manipulation actions in a scene given the context  $(x, l)$ .

#### B. Scene Representation

The input observation  $x$  is a structured point-cloud (PCD) in the robot's base-frame. We get this by combining the inputs from a sequence of pre-defined scanning actions with respect to the robot's base-frame. This point cloud is then

preprocessed by voxelizing at a 1mm resolution to solely to remove any duplicate points from overlapping camera views. This preprocessed pointcloud is then used as input into both  $\pi_I$  and  $\pi_R$ .

For  $\pi_I$ , we perform a second voxelization, this time at 5mm resolution. This creates the downsampled set of points  $P$ , such that the interaction point  $p_I \in P$ . This means  $\pi_I$  has a consistently high-dimensional input and action space - for a robot looking at its environment with a set of  $N$  aggregated observations, this can be 5000-8000 input "tokens" representing the scene.

While we're still discretizing the world for  $\pi_I$  similar to prior work [19], [20], [2], we voxelize at a higher resolution to capture fine local details even in large scenes. Usually, such a representation can be computationally inefficient to learn from, but we couple this with a set-based learning formulation which allows us to attend to fine details in a data efficient manner.

#### C. Interaction Prediction Module

We use our insight about tasks being shaped around an interaction point to make learning more robust and more efficient: instead of predicting the agent's motion directly, we formulate our  $\pi_I$  to solely focus on predicting a specific point  $p_I \in P$ , representing a single 5mm voxel that is referred to as the "interaction point". This formulation is akin to learning object affordance, and can be thought of similar to prior work like Transporter Nets in 2D [6]. We hypothesize that predicting an attention directly on visual features, even for manipulation actions, will make SLAP more general.

Our interaction prediction module takes in the triplet  $(x, P, l)$  describing the current task. The output is a score assignment to each point in  $P$  indicating whether it is an interaction point for  $l$ . We take the *argmax* of this score as the resulting interaction point,  $p_I \in SE(3)$ .

Since we have multiple modalities in our input we use a PerceiverIO [22] backbone to process the data. We chose the

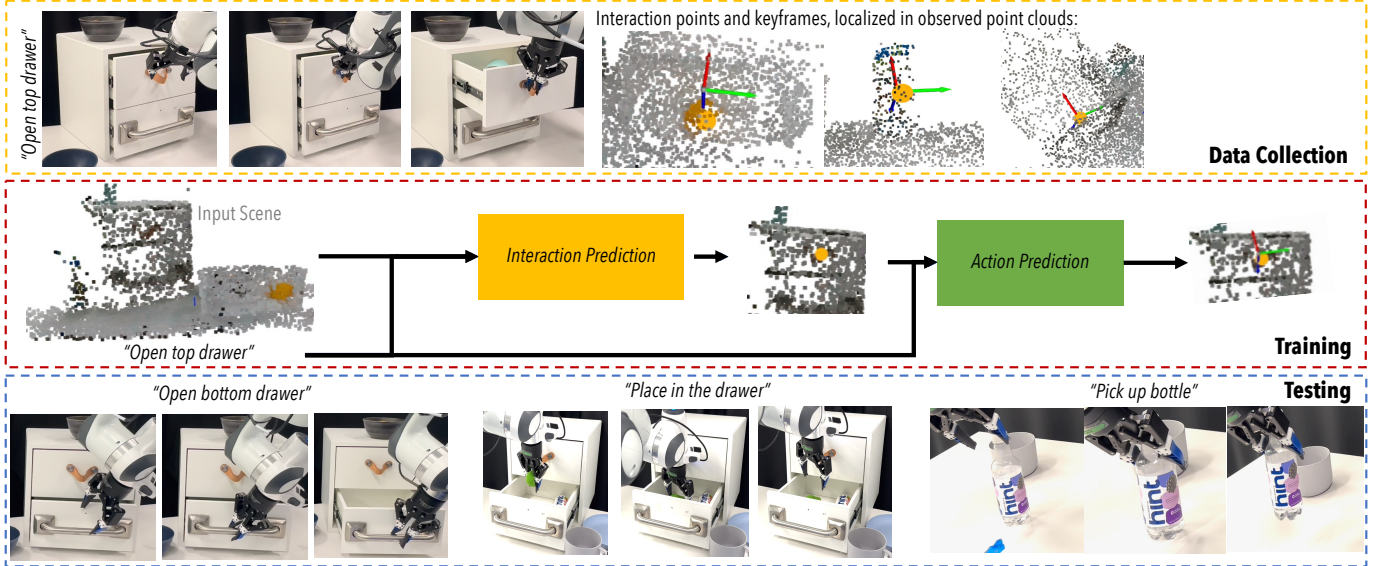


Fig. 3: Illustration of the complete process for training SLAP. Demonstrations are collected and used to train the Interaction Prediction module and the Action Prediction Module separately. Thus, we can make predictions as to where the robot should move next, based on the predicted interaction point.

PerceiverIO transformer based on prior work on language-conditioned real world policies [2], but also note that it has an important quality for us: it uses a fixed-size latent space, which allows us to handle a very large, variable input space.

We first pass our input point cloud through two *modified set abstraction* layers [4] which result in a sub-sampled point-cloud with each point’s feature capturing the local spatial structure around it at two different resolutions. This is to encourage the classifier to pay attention to *local structures* rather than a specific point which might or might not be visible in real-world settings. The natural language command is tokenized using the CLIP encoder [23] and added to the encoded point cloud to create an input sequence. We use cosine-sine positional encodings to distinguish between PCD tokens and language tokens and pass them to the PerceiverIO transformer. Each point  $i \in P$  in the point cloud is assigned a score with respect to task  $\tau_j$  which results in the interaction point for that task,  $p_I^j$ :

$$p_I^j = \operatorname{argmax}_{x,y,z} (S(i = p_I^j | l, x, P, \mathcal{D}^j)) \quad (1)$$

where  $\mathcal{D}^j$  is the set of expert demonstrations provided for task  $\tau_j$ . The IPM architecture overview is provided in Fig. 2.

**Modified Set Abstraction Layer.** The default SA layer as introduced by Qi et al. [4] uses farthest point sampling (FPS) to determine which locations feature vectors are created. FPS ensures that subsampled point-cloud is a good representation of a given scene, without any guarantees about the granularity. However, it’s very sensitive to the number of points selected - in most Pointnet++-based policies, a fixed number of points are chosen using FPS [4]. In this work, however, we want to adapt to scenes which can be of varying sizes, possibly with multiple views, and guarantee we will not miss small details. To this end, we propose an alternative version of

the PointNet++ set abstraction layer, which uses an *evenly* downsampled point cloud, where points are placed at some fixed resolution, wherever points have been observed – giving us a downsampled set of points  $P$ . This guarantees we can attend even to small features, and allows us to predict an interaction point  $p_I$  from the set of PointNet++ aggregated features.

**Supervision.** Each task is described by 3 actions which are tagged manually by an expert while providing a kinesthetic demonstration. We choose the action associated with the first gripper change exceeding a threshold as the expert interaction point  $\hat{p}_I$ . This is a simple heuristic which can be applied automatically. Due to the use of the modified set abstraction layer above, even though the number of input points can vary from observation to observation, we can always predict a reasonable  $p_I$ . The training of this module is further described in Sec. III-G.

**Visualizing the Learned Attention.** Since we use scores to choose the final interaction point, our classifier model is naturally interpretable, being able to highlight points of interest in a scene. We visualize this attention by selecting the points with the highest 5% of interaction score given a language command  $l$ . See Fig. 8 for examples.

#### D. Relative Action Module

The relative action module relies on the interaction point predicted by the classifier and operates on a cropped point cloud,  $x_R$ , around this point to predict the actions associated with this sequence. As in the interaction prediction module, the model uses a cascade of modified *set abstraction* layers as the backbone to compute a multi-resolution encoding feature over the cropped point cloud. We train three multi-head regressors (described further below) over these features to predict the actions,  $\{a_a, a_i, a_d\}$  for the overall task (see Fig. 4). Positions

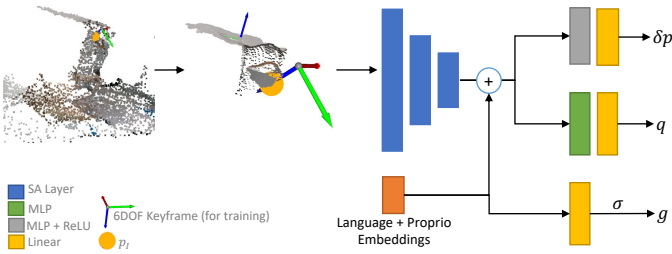


Fig. 4: Regression model architecture with separate heads for each output. The point-cloud is cropped around the interaction point with some perturbation and passed to a cascade of set abstraction layers. Encoded spatial features are then passed to two different MLPs, which are then fed into two separate linear layers which predict the delta end-effector position and orientation.  $g$  is predicted based solely on proprioception information.

and orientations associated with the interaction action generally tend to be much closer to the crop-center thus we train one model per action to encourage each action to be learned according to its own distribution.

Also note that the cropped input point-cloud is not perfectly centered at the ground truth interaction point  $\hat{p}_I$ , but rather with some noise added:  $\hat{p}_I' = \hat{p}_I + \mathcal{N}(0, \sigma)$ . This is done to force the action predictor to be robust to sub-optimal interaction point predictions by the interaction predictor module during real-world roll-outs.

Specifically,  $\pi_R$  has three heads, one for each component of the relative action space: gripper activation  $g$ , position offset  $\delta p$  and orientation  $q$ . Thus for each part of the action sequence, the keyframe position is calculated as:  $p = p_I + \delta p$ . When acting, the robot will move to  $(p, q)$  via a motion planner, and then will send a command to the gripper to set its state to  $g$ .

### E. Providing Demonstrations

For each episode, we first scan the scene with a pre-defined list of scanning positions to collect an aggregated  $x$ . In our case, we make no assumption as to what these are, or how large the resulting input point cloud  $x$  is.

Then, we collect demonstration data using kinesthetic teaching. The demonstrator physically moves the arm through the trajectory associated with each task, recording the *keyframes* [24] associated with action execution. These represent the salient moments within a task – the bottlenecks in the tasks’ state space, which can be connected by our low-level controller.

At each keyframe, we record the associated expert action  $\hat{a} = (\delta p, \hat{q}, \hat{g})$ . We don’t look at the problem of learning to connect these actions with a low level controller in this work, but instead assume that low-level controllers exist - in our case we use Polymetis [25]. Examples of tasks studies in this work are shows in Fig. 5.

### F. Data Processing

We execute each individual task open-loop based on an initial observation. We use data augmentation to make sure even

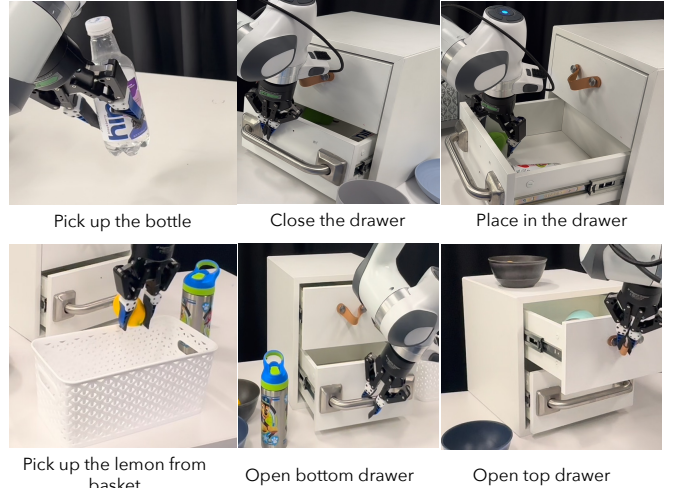


Fig. 5: Examples of tasks executed on a Franka arm through our trained model in a clean setting. Our approach supports training on a wide range of tasks both in clean and cluttered settings, and generalizes well to object locations, using minimal real-world data.

with relatively few examples, we still see good generalization performance.

**Data Augmentation.** Prior work in RGB-D perception for robotic manipulation (e.g. [26], [27]) has extensively used a variety of data augmentation tricks to improve real-world performance. In this work, we use three different data augmentation techniques to randomize the input scene  $x$  used to train  $p_I = \pi_I(x, l)$ :

- *Elliptical dropout*: Random ellipses are dropped out from the depth channel to emulate occlusions and random noise, as per prior work [28], [26]. Number of ellipses are sampled from a Poisson distribution with mean of 10.
- *Additive Noise*: Gaussian process noise is added to the points in the point-cloud. Parameters for the Gaussian distribution are sampled uniformly from given ranges. This is to emulate the natural frame-to-frame point-cloud noise that occurs in the real-world.
- *Rotational Randomization*: Similar to prior work [2], [29], [30], we rotate our entire scene around the z-axis within a range of  $\pm 45$  degrees to help force the model to learn rotational invariance.
- *Random cropping*: with  $p = 0.75$ , we randomly crop to a radius around  $\hat{p}_I + \delta$ , where  $\delta$  is a random positional offset sampled from a Gaussian distribution. The radius to crop is randomly sampled in  $(1, 2)$  meters.

**Data Augmentation for  $\pi_R$ .** We crop the relational input  $x_R \subset x$  around the ground-truth  $p_I$ , using a fixed radius  $r = 0.1m$ . We implement an additional augmentation for learning our action model. Since  $p_I$  is chosen from the discretized set of downsampled points  $P$ , we might in principle be limited to this granularity of response. Instead, we randomly shift both  $p_I$  and the positional action  $\delta p$  by some uniformly-sampled offset  $\delta r \in \mathbb{R}^3$ , with up to  $0.025m$  of noise. This lets  $\pi_R$  adapt to interaction prediction errors of up to several centimeters.

### G. Training the Interaction Prediction Module

We train  $\pi_I$  with a cross-entropy loss, predicting the interaction point  $p_I$  from the downsampled set of coarse voxels  $P$ . We additionally apply what we call a *locality loss* ( $L_{loc}$ ). Conceptually, we want to penalize points the further they are from the contact point, both to encourage learning relevant features as well as to aid in ignoring distractors. To achieve this, we define the locality loss as:

$$L_{loc} = \sum_{k \in P} \text{softmax}(f_k) \|\hat{p}_I, k\|^2 \quad (2)$$

where  $f_k$  is the output of the transformer (before the sigmoid) for point  $k \in P$ . The *softmax* turns  $f_k$  into an attention over the points, meaning that  $L_{loc}$  can be interpreted as a weighted average of the square distances. Points further from  $\hat{p}_I$  are therefore encouraged to have lower classification scores.

Combining our two losses, we obtain:

$$L_I = CE(P, \hat{p}_I) + \frac{w}{|P|} L_{loc} \quad (3)$$

where  $w$  is a scaling constant that implicitly defines how much spread to allow in our points.

### H. Training the Relative Action Module

We train  $a = (p, q, g) = \pi_R(x_R)$  with an L2 loss over the  $\delta p$ , and we use a quaternion distance metric for the loss on  $g$ . Following [?] for the orientation, we can compute the angle between two quaternions  $\theta$  as:

$$\theta = \cos^{-1}(2\langle \hat{q}_1, \hat{q}_2 \rangle^2). \quad (4)$$

We can remove the cosine component and use it as a squared distance metric between 0 and 1. We then compute the position and orientation loss as:

$$L_R = \lambda_p \|\delta p - \hat{\delta p}\|_2^2 + \lambda_q (1 - \langle \hat{q}, q \rangle) \quad (5)$$

where  $\lambda_p$  and  $\lambda_q$  are weights on the positional and orientation components of the loss, set to 1 and  $1e-2$  respectively.

Predicting gripper action is a classification problem trained with a cross-entropy loss. For input we use proprioceptive information about the robot as input, i.e.  $s = (g_{act}, g_w, ts)$  where  $g_{act}$  is 1 if gripper is closed and 0 otherwise,  $g_w$  is the distance between fingers of the gripper and  $ts$  is the time-step in the task. Gripper action is Sigmoid over a simple linear layer and MLP over  $s$ . The gripper action loss is then:

$$L_g = \lambda_g CE(g, \hat{g}) \quad (6)$$

where  $\lambda_g$  is the weight on cross-entropy loss set to 0.0001. The batch-size is set at 1 for this implementation.

We train  $\pi_I$  and  $\pi_R$  separately for  $n = 85$  epochs. At each epoch, we compare validation performance to the current best - if validation did not improve, we reset performance to the last best model.

## IV. EXPERIMENTS

### A. Task and Object Setup

We report the success rate of our model for 8 real-world tasks shown in Table I, and compare it against prior baselines trained using the same labeling scheme. Overall, we see an improvement of 30% over our best comparative baseline - PerAct [2]. We used the same objects for each version of the task, but different background distractors may appear in the out-of-distribution experiments shown in Table II. Success for opening drawers is if the drawer is 50% open after execution; this is because sometimes the drawer is too close to the robot's base for it to open fully.

**Testing Methodology.** We test each model under two different conditions:

- In-distribution scenes; i.e. those with seen distractor objects and objects placed roughly in the same range of positions and orientations as in the training data.
- Out-of-distribution scenes; i.e. those with unseen distractors and the implicated object placed significantly out of the range of positions and orientations already seen.

We run 5 tests per scene per model and report the percentage success numbers in Table I and Table II. Note that our in-distribution terminology means a set of unseen scenes which only include previously seen objects. The in-distribution and out-of-distribution sets of objects used in this study are presented in Fig. 6.

**Baselines.** We compare our model against the Perceiver-Actor (PerAct) agent from [2]. We use PerAct as presented in the paper, i.e. one model for all tasks and actions. We train each model for the same number of training steps and choose the SLAP model based on the best validation loss. For PerAct, we use the last checkpoint, per their testing practices [2].

**Language Analysis.** Our hypothesis is that by using pre-trained CLIP language embeddings to learn our spatial attention module  $\pi_I$ , our model can generalize to unseen language to some extent. We test this by running an experiment where we evaluate performance on in-distribution scene settings, prompted by a held-out list of language expressions. We choose three representative tasks for this experiment and run 10 tests with 2 different language phrasings.

**Model Design Analysis by Ablation.** We evaluate the effect of design decision like cropping around the interaction point and providing the interaction point to the APM. We compare SLAP against PerAct and the following ablations on three different tasks:

- 1) Optimal IPM SLAP: APM gets cropped scene around ground truth interaction point
- 2) “No-crop” SLAP: APM gets the entire scene and predicts with respect to interaction point
- 3) PointNet++ Policy: Equivalent to APM getting the entire scene, without any notion of an interaction point

We report the distance error between the predicted action and the ground truth action.

**Analysis of Data Augmentation.** We hypothesize that SLAP with data augmentation helps with accurate prediction

of the interaction point compared to SLAP without data augmentation. We test this hypothesis under two conditions:

- 1) *Without clutter training data*: training data consists of single-object environments with only the relevant object for the given task
- 2) *With clutter training data*: training data consists of multiple objects where there are multiple distractors in the scene

Success indicates that the IPM was able to correctly predict the interaction point on the correct part of the object. Note that this metric is notably different from the distance error metric. For example, for the “open top drawer” task, the IPM can predict an interaction point close to the handle of drawer but on the face of the drawer rather than the handle and this may lead to failure. This metric measures the IPM’s ability to generalize its understanding of task affordances.

### Results

**Hybrid vs Monolithic Architecture.** For the same number of epochs, our model does better than PerAct on 6 out of 8 tasks when tested in in-distribution setting (Table I) and 5 out of 8 tasks when tested in out-of-distribution setting (Table II). PerAct performs equally well as our model for 2 out of 8 tasks on our in-distribution scenes. Similarly, for our “hard” generalization scenes, PerAct performed equally well in two cases, and actually outperformed SLAP when picking up a bottle. For SLAP, the biggest failure mode for in-distribution settings was prediction of an incorrect attention point. While our approach is robust to small variations in attention point, if it is too large,  $\pi_R$  will not be able to adapt. In these cases,  $\pi_R$  predicted the correct trajectory, but not with respect to the right part of the object, leading to failures.

**Model Design Ablations.** Our results suggest that providing the interaction point to the APM is the key reason why SLAP performs better than baselines and also learns faster (Table IV). SLAP is capable of predicting actions with high accuracy (1.6cm error) even with up to 5cm average error in the prediction of interaction point (first column). The “No-crop” SLAP variant performs just as well as baseline SLAP. However, the PointNet++ policy has the highest amount of error across all the models. This indicated that predicting actions with respect to the interaction point is the key reason for lower error rates in SLAP.

**Data Augmentation.** We see a categorical improvement in SLAP’s ability to predict the interaction point on the correct object feature (Table V). We also see a significant drop in prediction performance of the model when we add clutter to existing training sets of 6 tasks and 9 tasks *without data augmentation*. Thus our data augmentation techniques help the IPM better understand scene structure and robustly predict the interaction point.

**Out-of-Distribution Scene Generalization.** We see a significant drop in the success rate for both PerAct and SLAP when tested on out-of-distribution settings. For PerAct, we would often see correct approach actions, but then it would fail to predict the right interaction. With SLAP, however, we



Fig. 6: Within distribution objects used at training time and out-of-distribution objects introduced during testing in our experiments.

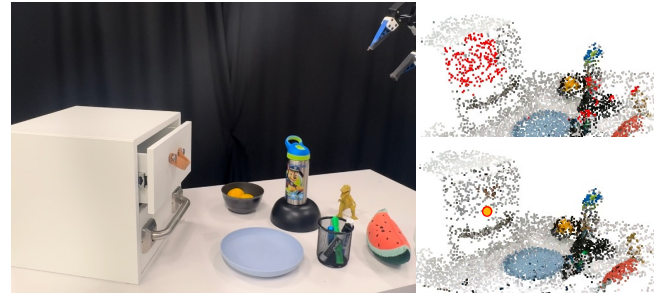


Fig. 7: An out-of-distribution SLAP failure example where an extreme sideways configuration of the drawer is paired with unseen distractors for the “open top drawer” skill. We can see the attention mask ranking other distractors in its top 5% and failing to choose an optimal interaction point.

saw that  $p_I$  was predicted fairly accurately, but the regressor would fail for out-of-distribution object placements specifically because of bad orientation prediction. When  $\pi_I$  failed, it was because the position and orientation of the target object was dramatically different, *and* there were unseen distractors which confused it, see example in Fig. 7.

**Language Generalization.** We don’t specifically focus on language generalization in this paper, but we show that even with a relatively small amount of language, we can show some transfer to new, notably different commands. We see similar a success rate to out-of-distribution scene experiments for “pick up the bottle” and “open top drawer” tasks. However, we observe that the “place into drawer” task’s success rate drops significantly. We also observe that the relevant action prediction module weighs the input scene’s structure as more important than the language by itself. For example, the edge of the drawer chosen as interaction point with phrasing “add to the drawer” results in closing of the drawer action.

**Qualitative Results on Stretch.** We trained a single-task model for the Stretch robot that can learn a tabletop task of “picking up the bottle” with just five demonstrations. During training and testing, the robot was spawned within arm-length distance of the table. Since our model learns to predict actions relative to the scene, we observed the robot executing behaviors that were never demonstrated. We found that the robot could move its base and re-orient itself to

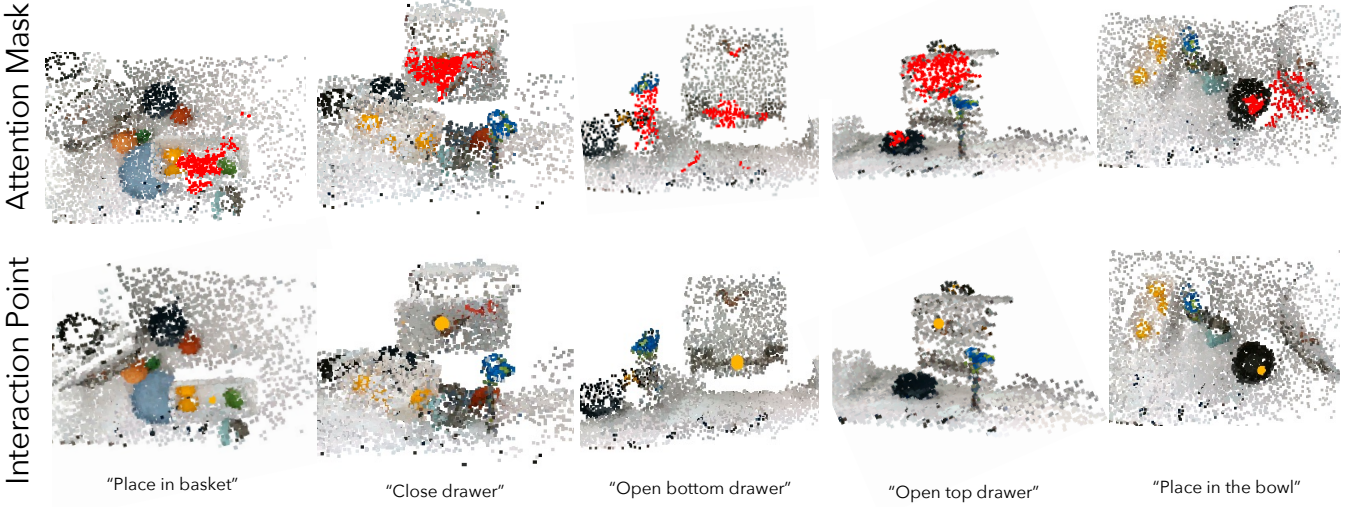


Fig. 8: Predicted mask (red) and interaction sites (yellow sphere) for five tasks.

Task Name	SLAP (ours)	PerAct [2]
Open bottom drawer	<b>80%</b>	00%
Open top drawer	<b>80%</b>	60%
Close drawer	<b>100%</b>	<b>100%</b>
Pick lemon from basket	<b>80%</b>	60%
Pick bottle	<b>60%</b>	<b>60%</b>
Place into the drawer	<b>80%</b>	60%
Place into the basket	<b>100%</b>	40%
Place into the bowl	<b>60%</b>	40%
Total Success Rate	80%	50%
Improvement		+30

TABLE I: Performance of SLAP versus PerAct on previously unseen real-world scenes, restricted only to “in-distribution” configurations of objects. SLAP is as good as or better than the baselines for all tasks.

Task Name	SLAP (ours)	PerAct [2]
Open bottom drawer	<b>60%</b>	00%
Open top drawer	<b>40%</b>	<b>40%</b>
Close drawer	<b>40%</b>	<b>40%</b>
Pick lemon from basket	<b>40%</b>	10%
Pick bottle	40%	<b>60%</b>
Place into the drawer	<b>60%</b>	40%
Place into the basket	<b>60%</b>	10%
Place into the bowl	<b>40%</b>	00%
Average	47.5%	27.5%
Improvement		+20

TABLE II: Performance of our best-validation score model on real-world instances against PerAct for both in- and out-of-distribution settings. The highest success rate in each row is bolded. Notably, while SLAP improves generalization to out-of-distribution scenes, it still isn’t fully robust to variations in the observed point cloud.

pick up the object when placed at novel offset positions relative to the object during testing. This indicates that our method generalizes to novel positions of the robot as long as the action representation can capture feasible positions and

Task Name	Success rate
Pick up the bottle	40%
Open top drawer	40%
Place inside the drawer	20%

TABLE III: Success rates when above listed tasks are prompted with in-distribution scenes and language sampled from a held-out set of phrasings.

orientations. We also found that transferring the model trained on data from Franka to Stretch resulted in subpar prediction performance due to differences in camera viewpoints. We plan to explore additional augmentations, such as frame drop-outs, to improve our training methodology for transferring models across different robot embodiments.

## V. DISCUSSION

Our experiments show that SLAP has a number of advantages over previous work. We also observe that SLAP predicted consistently successful actions for opening the top and bottom drawers. While the top drawer handle is a small leather loop, the bottom drawer handle is a slender cylindrical rod. PerAct produces more inaccurate predictions for the small loop on the drawer, while failing completely to grasp the bottom handle. See Fig. 9 for an example. We note that our  $\pi_I$  has a finer granularity than PerAct’s representation.

**Locality Loss.** We observed reduced object confusion with locality loss when comparing to a version of SLAP trained without it. Before adding the locality loss, the attention for a skill would be spread farther around the scene – spreading to the bottom drawer from top and vice-versa for example. This led to confusion and lower success rates on drawer-related tasks (previously, 0% on bottom drawer and 70% on top drawer from a 9-task model trained with data augmentation). However, the locality loss encouraged attention to be

Task Name	IPM Only	SLAP	Oracle IPM SLAP	No crop SLAP	PointNet++	PerAct
Close drawer	0.08	0.025	0.0146	0.015	0.071	0.016
Open top drawer	0.032	0.019	0.019	0.019	0.036	0.039
Place in basket	0.047	0.004	0.002	0.002	0.018	0.02
Average	0.053	0.016	0.012	0.012	0.042	0.025

TABLE IV: Distance error for predicted action reported for SLAP, ablations and PerAct. PointNet++ baseline does even worse than PerAct, indicating interaction point prediction being key to SLAP improvements.

Data Augmentation	Scene complexity		Without Clutter Training Data				With Clutter Training Data			
	Number of tasks		6 tasks		9 tasks		6 tasks		9 tasks	
	No	Yes	No	Yes	No	Yes	No	Yes	No	Yes
Open bottom drawer	58%	100%	22%	0%	0%	77%	66%	77%		
Open top drawer	69%	53.84%	77%	77%	44%	87%	66%	75%		
Pick up bottle	100%	100%	100%	78%	83%	100%	83%	100%		
Pick up toolbox	75%	58%	91%	78%	50%	91%	66%	66%		
Place in mug	75%	83.3%	83%	75%	100%	83%	100%	75%		
Pick up the pear	<10%	100%	0%	0%	<10%	50%	0%	33%		
Close drawer	n/a	n/a	25%	41%	n/a	n/a	58%	66%		
Open toaster	n/a	n/a	76%	66%	n/a	n/a	56%	90%		
Place in drawer	n/a	n/a	66%	33%	n/a	n/a	25%	91%		
Average	63.66	82.52	60	49.78	47	81.33	57.78	74.78		

TABLE V: How the performance of SLAP scales: with or without data augmentation, with a varying number number of tasks, and with or without the addition of training data consisting of cluttered scenes. Scaling up the data includes both numeric complexity as well as semantic complexity; in the 9 task case, multiple tasks refer to the same object.

concentrated tightly on the relevant surfaces of the implicated object, as seen in Fig. 10.

## VI. CONCLUSION

In this work, we proposed a novel architecture which combines the *structure* of a point-cloud based input with *semantics* from language and accompanying demonstrations to predict continuous end-effector actions for manipulation tasks. A novel two-stream architecture - with a discrete *interaction prediction module* determining where an action will take place, and a continuous *relative action module* converting that into motions - allows us to have strong generalization to unseen scene configurations. Our model displays 80% success on 8 real-world tasks when tested on unseen scene configurations and 47.5% success rate in out-of-distribution settings, based only on 12 demonstrations for each task.

However, SLAP is not without its limitations. We find that our solution has high variance in out-of-distribution situations, resulting in complete failure if  $\pi_I$  fails to correctly identify the context. To address this, we plan to integrate pre-trained weights and context into  $\pi_I$  to make it more resilient to inter-object confusion. For  $\pi_R$ , we often encounter failures for object orientations outside of the training distribution, as it does not extrapolate orientations well. This can be improved by integrating heuristic or data-driven grasp models to enhance action grounding for new object configurations.

## REFERENCES

- [1] A. Brohan, N. Brown, J. Carbajal, Y. Chebotar, J. Dabis, C. Finn, K. Gopalakrishnan, K. Hausman, A. Herzog, J. Hsu *et al.*, “Rt-1: Robotics transformer for real-world control at scale,” *arXiv preprint arXiv:2212.06817*, 2022.
- [2] M. Shridhar, L. Manuelli, and D. Fox, “Perceiver-actor: A multi-task transformer for robotic manipulation,” *arXiv preprint arXiv:2209.05451*, 2022.
- [3] D. Driess, F. Xia, M. S. Sajjadi, C. Lynch, A. Chowdhery, B. Ichter, A. Wahid, J. Tompson, Q. Vuong, T. Yu *et al.*, “Palm-e: An embodied multimodal language model,” *arXiv preprint arXiv:2303.03378*, 2023.
- [4] C. R. Qi, L. Yi, H. Su, and L. J. Guibas, “Pointnet++: Deep hierarchical feature learning on point sets in a metric space,” *Advances in neural information processing systems*, vol. 30, 2017.
- [5] W. Yuan, C. Paxton, K. Desingh, and D. Fox, “Sornet: Spatial object-centric representations for sequential manipulation,” in *Conference on Robot Learning*. PMLR, 2022, pp. 148–157.
- [6] A. Zeng, P. Florence, J. Tompson, S. Welker, J. Chien, M. Attarian, T. Armstrong, I. Krasin, D. Duong, V. Sindhwani *et al.*, “Transporter networks: Rearranging the visual world for robotic manipulation,” in *Conference on Robot Learning*. PMLR, 2021, pp. 726–747.
- [7] M. Shridhar, L. Manuelli, and D. Fox, “Cliport: What and where pathways for robotic manipulation,” in *Conference on Robot Learning*. PMLR, 2022, pp. 894–906.
- [8] C. Huang, O. Mees, A. Zeng, and W. Burgard, “Visual language maps for robot navigation,” *arXiv preprint arXiv:2210.05714*, 2022.
- [9] S. James and A. J. Davison, “Q-attention: Enabling efficient learning for vision-based robotic manipulation,” *IEEE Robotics and Automation Letters*, vol. 7, no. 2, pp. 1612–1619, 2022.
- [10] M. Ahn, A. Brohan, N. Brown, Y. Chebotar, O. Cortes, B. David, C. Finn, K. Gopalakrishnan, K. Hausman, A. Herzog *et al.*, “Do as i can, not as i say: Grounding language in robotic affordances,” *arXiv preprint arXiv:2204.01691*, 2022.
- [11] K. Mo, L. J. Guibas, M. Mukadam, A. Gupta, and S. Tulsiani, “Where2act: From pixels to actions for articulated 3d objects,” in *Proceedings of the IEEE/CVF International Conference on Computer Vision*, 2021, pp. 6813–6823.
- [12] A. Hundt, B. Killeen, N. Greene, H. Wu, H. Kwon, C. Paxton, and G. D. Hager, ““Good robot!”: Efficient reinforcement learning for multi-step visual tasks with sim to real transfer,” *IEEE Robotics and Automation Letters*, vol. 5, no. 4, pp. 6724–6731, 2020.
- [13] P.-L. Guhur, S. Chen, R. Garcia, M. Tapaswi, I. Laptev, and C. Schmid, “Instruction-driven history-aware policies for robotic manipulations,” *arXiv preprint arXiv:2209.04899*, 2022.

[14] X. Zhou, R. Girdhar, A. Joulin, P. Krähenbühl, and I. Misra, “Detecting twenty-thousand classes using image-level supervision,” in *ECCV*, 2022.

[15] I. Misra, R. Girdhar, and A. Joulin, “An end-to-end transformer model for 3d object detection,” in *Proceedings of the IEEE/CVF International Conference on Computer Vision*, 2021, pp. 2906–2917.

[16] R. Wu, Y. Zhao, K. Mo, Z. Guo, Y. Wang, T. Wu, Q. Fan, X. Chen, L. Guibas, and H. Dong, “Vat-mart: Learning visual action trajectory proposals for manipulating 3d articulated objects,” *arXiv preprint arXiv:2106.14440*, 2021.

[17] Z. Xu, Z. He, and S. Song, “Umpnet: Universal manipulation policy network for articulated objects,” *arXiv preprint arXiv:2109.05668*, 2021.

[18] O. Mees, J. Borja-Diaz, and W. Burgard, “Grounding language with visual affordances over unstructured data,” *arXiv preprint arXiv:2210.01911*, 2022.

[19] V. Blukis, C. Paxton, D. Fox, A. Garg, and Y. Artzi, “A persistent spatial semantic representation for high-level natural language instruction execution,” in *Conference on Robot Learning*. PMLR, 2022, pp. 706–717.

[20] S. Y. Min, D. S. Chaplot, P. Ravikumar, Y. Bisk, and R. Salakhutdinov, “Film: Following instructions in language with modular methods,” *arXiv preprint arXiv:2110.07342*, 2021.

[21] N. M. M. Shafullah, C. Paxton, L. Pinto, S. Chintala, and A. Szelam, “Clip-fields: Weakly supervised semantic fields for robotic memory,” *arXiv preprint arXiv:2210.05663*, 2022.

[22] A. Jaegle, S. Borgeaud, J.-B. Alayrac, C. Doersch, C. Ionescu, D. Ding, S. Koppula, D. Zoran, A. Brock, E. Shelhamer *et al.*, “Perceiver io: A general architecture for structured inputs & outputs,” *arXiv preprint arXiv:2107.14795*, 2021.

[23] A. Radford, J. W. Kim, C. Hallacy, A. Ramesh, G. Goh, S. Agarwal, G. Sastry, A. Askell, P. Mishkin, J. Clark *et al.*, “Learning transferable visual models from natural language supervision,” in *International Conference on Machine Learning*. PMLR, 2021, pp. 8748–8763.

[24] B. Akgun, M. Cakmak, J. W. Yoo, and A. L. Thomaz, “Trajectories and keyframes for kinesthetic teaching: A human-robot interaction perspective,” in *Proceedings of the seventh annual ACM/IEEE international conference on Human-Robot Interaction*, 2012, pp. 391–398.

[25] Y. Lin, A. S. Wang, G. Sutanto, A. Rai, and F. Meier, “Polymetis,” <https://facebookresearch.github.io/fairo/polymetis/>, 2021.

[26] C. Xie, Y. Xiang, A. Mousavian, and D. Fox, “Unseen object instance segmentation for robotic environments,” *IEEE Transactions on Robotics*, vol. 37, no. 5, pp. 1343–1359, 2021.

[27] A. Handa, A. Allshire, V. Makoviychuk, A. Petrenko, R. Singh, J. Liu, D. Makoviichuk, K. Van Wyk, A. Zhurkevich, B. Sundaralingam *et al.*, “Dextreme: Transfer of agile in-hand manipulation from simulation to reality,” *arXiv preprint arXiv:2210.13702*, 2022.

[28] J. Mahler, J. Liang, S. Niyaz, M. Laskey, R. Doan, X. Liu, J. A. Ojea, and K. Goldberg, “Dex-net 2.0: Deep learning to plan robust grasps with synthetic point clouds and analytic grasp metrics,” *arXiv preprint arXiv:1703.09312*, 2017.

[29] C. Paxton, C. Xie, T. Hermans, and D. Fox, “Predicting stable configurations for semantic placement of novel objects,” in *Conference on Robot Learning*. PMLR, 2022, pp. 806–815.

[30] W. Liu, C. Paxton, T. Hermans, and D. Fox, “Structformer: Learning spatial structure for language-guided semantic rearrangement of novel objects,” in *2022 International Conference on Robotics and Automation (ICRA)*. IEEE, 2022, pp. 6322–6329.

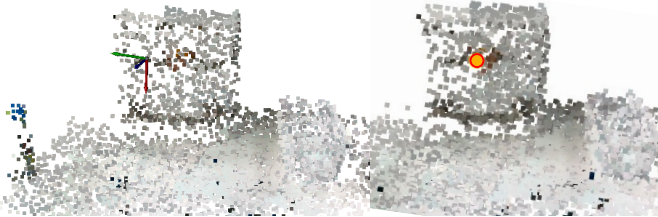


Fig. 9: Output for interaction action predicted by PerAct (left) and interaction point predicted by SLAP (right) for the same input. We see a trend where  $\pi_I$  predictions for finer details are consistently more optimal

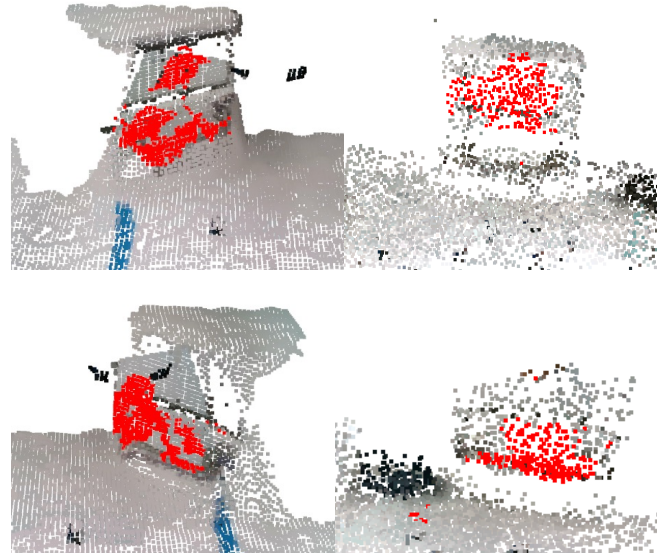


Fig. 10: A comparison of attention masks with (right) and without (left) the locality loss. Attention is more focused on relevant structures and less spread to irrelevant structures in the right image. The top row shows the attention mask for opening the top drawer: the previous model (left) spreads attention to the bottom handle due to its association with the “open” skill, while the new model (right) focuses only on the top drawer. Attention is more concentrated on handle for the “open bottom drawer” skill in the bottom row.

## APPENDIX

### A. Tasks

Every real-world task scene had a sub-sample of all within-distribution objects.

#### 1) Open the top drawer

- *Task*: Grab the small loop and pull the drawer open. Drawer configuration within training data is face-first with slight orientation changes
- *Action labeling*: Approach the loop, grab the loop, pull the drawer out
- *Success metric*: When the drawer is open by 50% or more

#### 2) Open the bottom drawer

- *Task*: Grab the cylindrical handle and pull the drawer open. Drawer configuration within training data is face-first with slight orientation changes. Note significantly different grasp required than for top drawer
- *Action labeling*: Approach the handle, grab it, pull the drawer out
- *Success metric*: When the drawer is open by 50% or more

#### 3) Close the drawer

- *Task*: This task is unqualified, i.e. the instructor does not say whether to close the top or bottom drawer instead the agent must determine which drawer needs closing from its state and close it. Align gripper with the front of whichever drawer is open and push it closed. The training set always has only one of the drawers open, in a front-facing configuration with small orientation changes
- *Action labeling*: Approach drawer from front, make contact, push until closed
- *Success metric*: When the drawer is closed to within 10% of its limit or when arm is maximally stretched out to its limit (when the drawer is kept far back)

#### 4) Place inside the drawer

- *Task*: Approach an empty spot inside the drawer and place whatever is in hand inside it
- *Action labeling*: Top-down approach pose on top of the drawer, move to make contact with surface and release the object, move up for retreat
- *Success metric*: Object should be inside the drawer

#### 5) Pick lemon from the basket

- *Task*: Reach into the basket where lemon is placed and pick up the lemon
- *Action labeling*:
- *Success metric*: Lemon should be in robot's gripper
- *Considerations*: Since the roll-out is open-loop and a lemon is spherical in nature, a trial was assigned success if the lemon rolled out of hand upon contact after the 2nd action. This was done consistently for both PerAct and SLAP.

#### 6) Place in the bowl

- *Task*: Place whatever is in robot's hand into the bowl receptacle
- *Action labeling*: Approach action on top of the bowl, interaction action inside the bowl with gripper open, retreat action on top of the bowl
- *Success metric*: The object in hand should be inside the bowl now

#### 7) Place in the basket

- *Task*: Place the object in robot's hand into the basket
- *Action labeling*: Approach action on top of the free space in basket, interaction action inside the basket with gripper open, retreat action on top of the basket
- *Success metric*: The object is inside the basket

#### 8) Pick up the bottle

- *Task*: Pick up the bottle from the table
- *Action labeling*: Approach pose in front of the robot with open gripper, grasp pose with gripper enclosing the bottle and gripper closed, retreat action at some height from previous action with grippers closed
- *Success metric*: The bottle should be in robot's gripper off the table

### B. Language Annotations

Below we include the list of language annotations used in our experiments. Table VI shows language that was used to train the model; we're able to show some robustness to different language expressions. We performed a set of experiments on held-out, out-of-distribution language despite this not being the focus of our work; this test language is shown in Table VII.

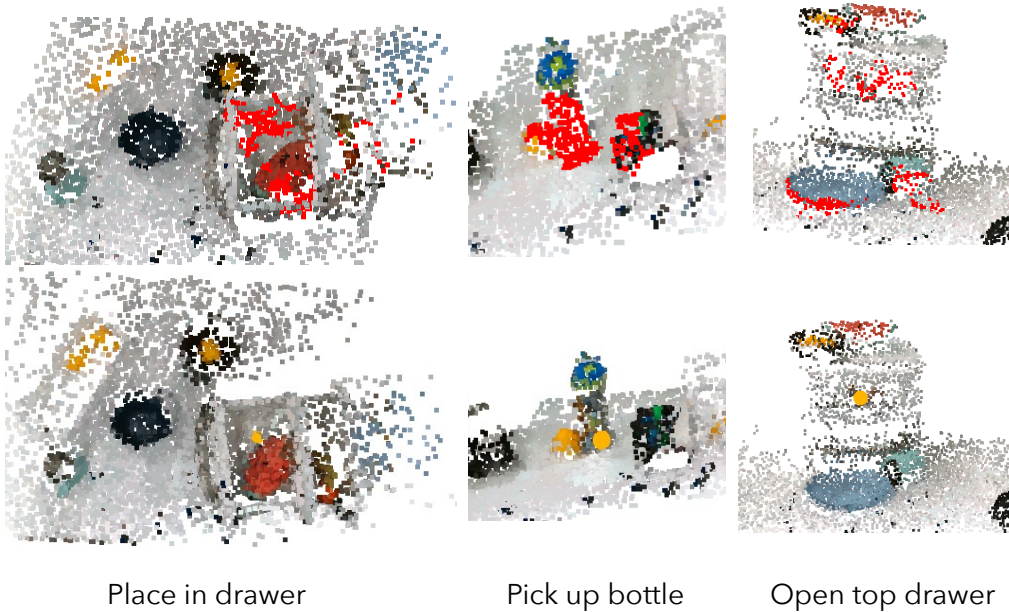


Fig. 11: Examples of out of distribution predictions made by  $\pi_I$ . We show that it is able to handle heavy clutter around the implicated object to predict interaction points. Note that the prediction for bottle picking is sub-optimal in this example.

### C. Out of distribution Results from SLAP

We show more results for attention point predicted by  $\pi_I$  in Fig. 11. For the placing task, the agent has never seen a heavily cluttered drawer inside before, but it is able to find flat space which indicates placing affordance. For the bottle picking task, this sample has a lemon right next to the bottle which changes the shape of the point-cloud around the bottle. We see that  $\pi_I$  is able to find an interaction point albeit with placement different from expert and lower down on the bottle. Similarly the open top drawer sample has more heavy clutter on and around the drawer to test robustness.

Fig. 12 shows the prediction and generated trajectory for picking up a previously unseen bottle. Note that while the models are able to detect the out of distribution bottle, the trajectory actually fails due to bottle being much wider and requiring more

Task Name	Training Annotations
pick up the bottle	pick up a bottle from the table pick up a bottle grab my water bottle
pick up a lemon	pick the lemon from inside the white basket grab a lemon from the basket on the table hand me a lemon from that white basket
place lemon in bowl	place the lemon from your gripper into the bowl add the lemon to a bowl on the table put the lemon in the bowl
place in the basket	place the object in your hand into the basket put the object into the white basket place the thing into the basket on the table
open bottom drawer	open the bottom drawer of the shelf on the table pull the second drawer out open the lowest drawer
close the drawer	close the drawers push in the drawer
open top drawer	close the drawer with your gripper open the top drawer of the shelf on the table pull the first drawer out open the highest drawer
place in the drawer	put it into the drawer place the object into the open drawer add the object to the drawer

TABLE VI: Examples of language used to train the model.

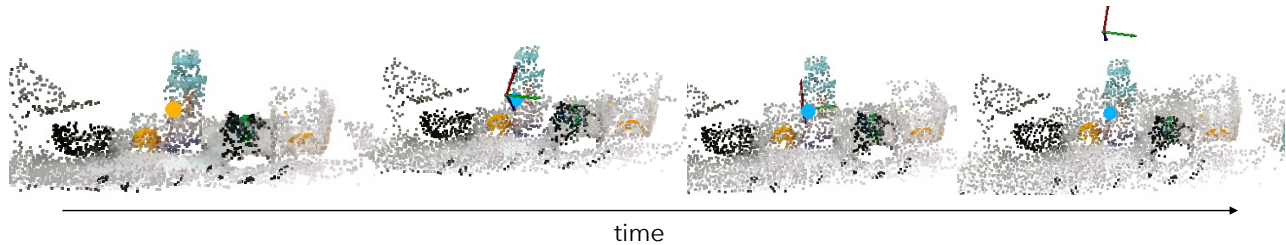


Fig. 12: A generalization example of success for our model. The new bottle has same shape as the within distribution bottle but is much taller, different in color and wider in girth. The model is able to predict the interaction site and a feasible trajectory around it. We note though the execution of this trajectory was a failure; due to wider girth of the bottle the predicted grasp was not accurate enough to enclose the object.

accuracy in grasping.

#### D. Motion Planning Failures

Our evaluation system has a simple motion planner which is not collision aware as a result we saw a number of task failures for both the models. However, we note that the frequency of task failures due to motion planning problems was higher for PerAct. We think it is because PerAct predicts each action of the same task as an entirely separate prediction trial, while SLAP forces continuity on the relative motions for the same task by centering them around the interaction point (see Fig. 12). That said, we also note with an advanced motion planner PerAct will not run into such issues as seen during our evaluations. Authors note in their own paper their heavy reliance on good motion planning solutions [2].

Task Name	Held-Out Test Annotations
Pick up the bottle	Grab the bottle from the table Pick up the water bottle
Open the top drawer	Pull top drawer out Open the first drawer
Place into the drawer	Add to the drawer Put inside the drawer

TABLE VII: Examples of out-of-distribution language annotations used for evaluation

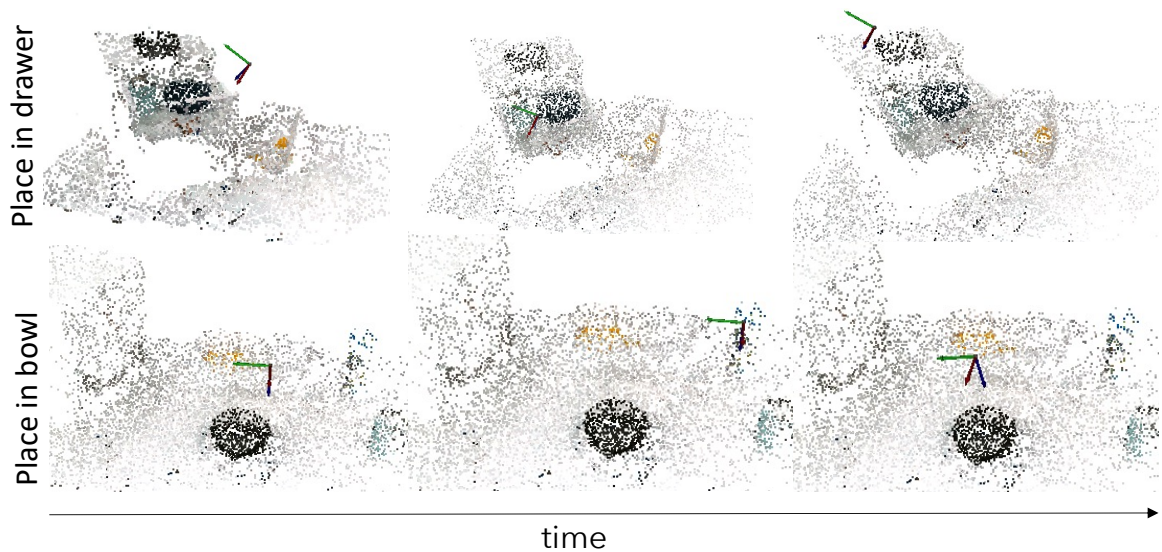


Fig. 13: Examples of failure cases for our baseline, PerAct, for the “place in drawer” and “place in bowl” tasks. In the top example, the gripper is moved from drawer’s side towards inside, instead of from the top as demonstrated by expert. The gripper ends up pushing off the drawer to the side as our motion-planner is not collision-aware. Note that SLAP does not exhibit such behaviors as  $\pi_R$  implicitly learns the collision constraints present in demonstrated data. In the bottom example, each action prediction is disjointed from previous and semantically wrong.